CPC(HEP & NP), 2012, **36**(11): 1106–1110 **Chinese Physics C** Vol. 36, No. 11, Nov., 2012

Simulation study of the parallax effect of gaseous detectors*

WANG Xiao-Hu(王小胡)[1,2] WU Jun-Long(吴军龙)[2] LI Jiang-Bo(李江波)[1]

[1] Fundamental Science on Nuclear Waste and Environmental Security Laboratory, Southwest University of Science and Technology, Mianyang 621010, China
[2] School of National Defense Science and Technology, Southwest University of Science and Technology; Mianyang 621010, China

Abstract: A simulation study of the parallax effect of gaseous detectors using the Garfield program is reported. A method that mainly uses non-uniform cathode potentials to reduce the parallax error of planar type gas detectors is described. By applying it to MWPC and Micro-pattern gas detectors, the method reduces the parallax broadening with very good results. For a 13° incidence track, the width (FWHM) of the parallax broadening is reduced to less than 20% of the normal one after using the special cathode potentials.

Key words: Garfield simulation, parallax error, gaseous detector

PACS: 29.40.Cs, 29.40.Gx **DOI:** 10.1088/1674-1137/36/11/012

1 Introduction

From the multi-wire proportional chamber (MWPC) [1] to micro-pattern detectors (MSGC [2], Micromegas [3], GEM [4]), gaseous detectors have played an important role in particle position detection. They are still widely used in high energy physics experiments, neutron & X-ray diffractions, etc. Most position sensitive gaseous detectors employ a planar structure, which has a uniform electric field perpendicular to the entrance window. For these detectors, parallax error is a major factor that deteriorates the precision of the detectors when measuring the position of the inclined incident neutral particles (X-ray or neutron). An effective way to reduce the effect of parallax errors is to produce arc-shaped or spherical-shaped detectors [5–7], but these special geometry detectors are obviously difficult to manufacture. In Ref. [8], the author introduced a new method to reduce the parallax broadening of an MWPC, which mainly employs a non-uniform (approximately Gaussian distribution) cathode potential to get a spherical electric field. An improvement in position resolution of up to nearly a factor of four was achieved by using this new parallax reducing technique.

In this paper, the Garfield [9] program is used to study the parallax effect of gaseous detectors. The principle of the parallax broadening reduction is to divide the electrode plane (a mostly cathode plane) into a family of separate electrodes, and the potential of each electrode is chosen according to its distance to the sample point, rather than employ a uniform potential. By our calculation, this method reduces the parallax error of the planar type gaseous detectors significantly.

2 Method

For planar type gaseous detectors, the parallax effect arises from the limited thickness of the sensitive volume and the uniform electric field that is perpendicular to the electrode planes. When an incidence particle enters the detector not perpendicularly to the entrance window, the electrons ionized by the particle will drift against the electric field to the anode plane, rather than move along the direction of the incidence particle. As a result, the measured position of the particle is not the same as the position the particle ought to arrive at on the anode plane. For an incidence beam with the same entrance angle not

---

Received 16 February 2012, Revised 23 March 2012

* Supported by Scientific Research Fund of the Sichuan Provincial Education Department (11ZA140) and Scientific Research Fund of Southwest University of Science and Technology (10zx7123)

perpendicular to the entrance window, a broadening of the measured position will occur, which is known as parallax broadening.

Since all incidence particles come from the sample position, the tracks of the particles are a series of radial lines. Therefore, for a parallax free detector, the electric field in the sensitive volume should not be uniform, but spherical instead. In this case, the ionized electrons can drift along the radial lines, which are consistent with the tracks of the incidence particles. Based on electromagnetic field theory, a negative point charge at the sample position can create a spherical electric field, and the potential around the point charge obeys the $U(r) \propto -1/r$ rule, where r is the distance between the interested point to the sample position. So, if the electrode planes of the detector are divided into a number of small separated units, and the potential of each unit is determined by the $U(r) \propto -1/r$ rule, a spherical electric field can be obtained.

In this paper, a detector with an active area of 20 cm × 20 cm, the total drift depth of 2 cm is studied. The distance from the detector window to the sample point is 40 cm, which corresponds to a maximum entrance angle of 13°, as shown in Fig. 1.

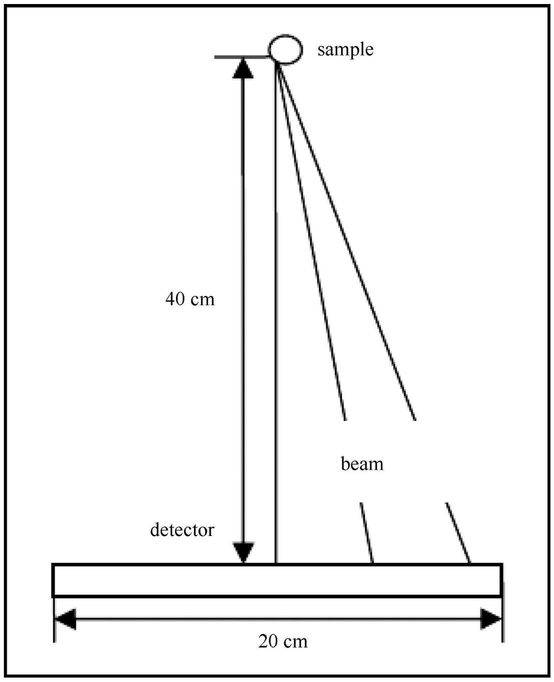

Fig. 1. Geometry of the detector setup.

Garfield was used to model the geometry of the detector. A set of parallel metal wires was chosen to form the cathode plane, and the potential of each cathode wire was determined according to its distance to the sample point based on the $U(r) \propto -1/r$ rule. Because of the parallax effect, for an inclined incident charged particle or a beam of inclined incident neutral particles, the arrival positions of the ionized electrons on the anode plane is a distribution. And the width of the distribution can be used to describe the effect of the parallax error. Therefore, the width (FWHM) of the position distribution of the ionized electrons from a charged particle was calculated, and was used as a representation of the parallax broadening.

3 Parallax error reduction for MWPC

3.1 Structural and Garfield modeling

In this paper, an MWPC with a non-symmetrical structure is studied. As shown in Fig. 2, the MWPC has a large drift region in the front part and a relatively small amplification region at the rear.

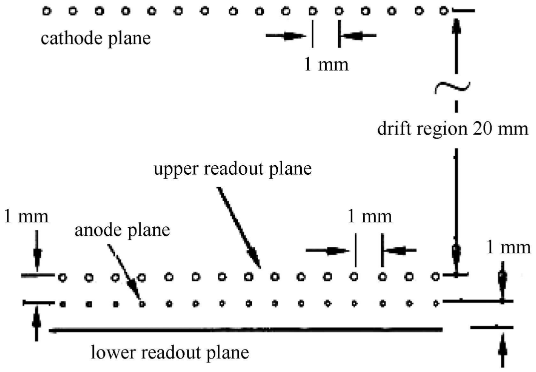

Fig. 2. Cell structure of the MWPC.

From the top down, the MWPC consists of a cathode plane, an upper readout plane, an anode plane, and a lower readout plane. The region from the cathode plane to the upper readout plane, which is named the drift region, had a thickness of 20 mm, and the spacing between the anode plane and each readout plane was 1 mm. All electrode planes are made of parallel metal wires with wire spacing of 1 mm. The diameters of the anode wires, cathode wires, and readout wires were 15 μm, 50 μm, and 20 μm, respectively. The anode plane was operated at a positive high voltage, and the readout planes were kept at earth potential. The cathode wires, however, were symmetrically divided into two groups, so as to obtain a better comparison. One group was normally operated at a uniform negative high voltage, while the other group was also operated at negative high voltage, but each wire had a potential corresponding to its distance to the sample position, according to the $U(r) \propto -1/r$ rule.

3.2 Simulation results

3.2.1 Electric field

The equipotential lines of the detector with special cathode high voltage are shown in Fig. 3. As can be seen, in the left part of the detector, where the cathode wires are operated in a same negative high voltage, the equipotential lines are uniform and parallel to the electrode planes. In the right part of the detector, where the potential of each wire corresponds to its distance to the sample position, the equipotential lines become approximately concentric arcs.

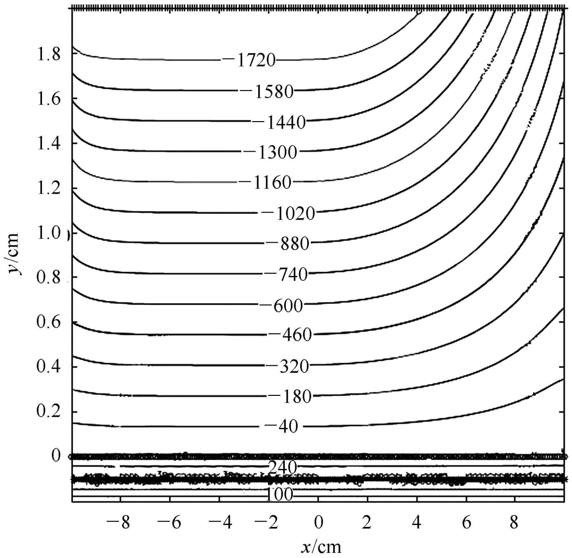

Fig. 3. Equipotential lines of the MWPC with special cathode potentials.

From the contour, we can deduce that the electric field in the left half of the detector is perpendicular to the electrode planes and the direction of the electric field in the right half of the detector becomes similarly radial from the sample point. Therefore, a similarly spherical electric field is obtained after applying special cathode wire potentials.

3.2.2 Electron drift lines from inclined tracks

As mentioned above, for a parallax free detector, the electrons will drift along the incidence track. So the width of the electron drift lines from a charged track can be used as the reflection of the parallax error. The electron drift lines for a charged particle with incidence angle of ±8° and ±13° are shown in Fig. 4. As can be seen, for the same incident angle, the width of the electron drift lines is much smaller in the special cathode potential region than in the normal cathode potential region. For example, for the 13° incident track, the ionized electrons in the normal electric field region spread to 5 anode wires on the a anode plane, but in the region with special cathode potentials, the ionized electrons are only concentrated on one anode wire. Obviously, the reduction of parallax broadening after using special cathode potentials is remarkable.

However, because of the anode wire modulation of the MWPC, the position distribution of the ionized electrons on the anode plane could not correctly represent for the parallax broadening of the detector. The reduction of parallax broadening using special cathode potentials could not be exactly calculated.

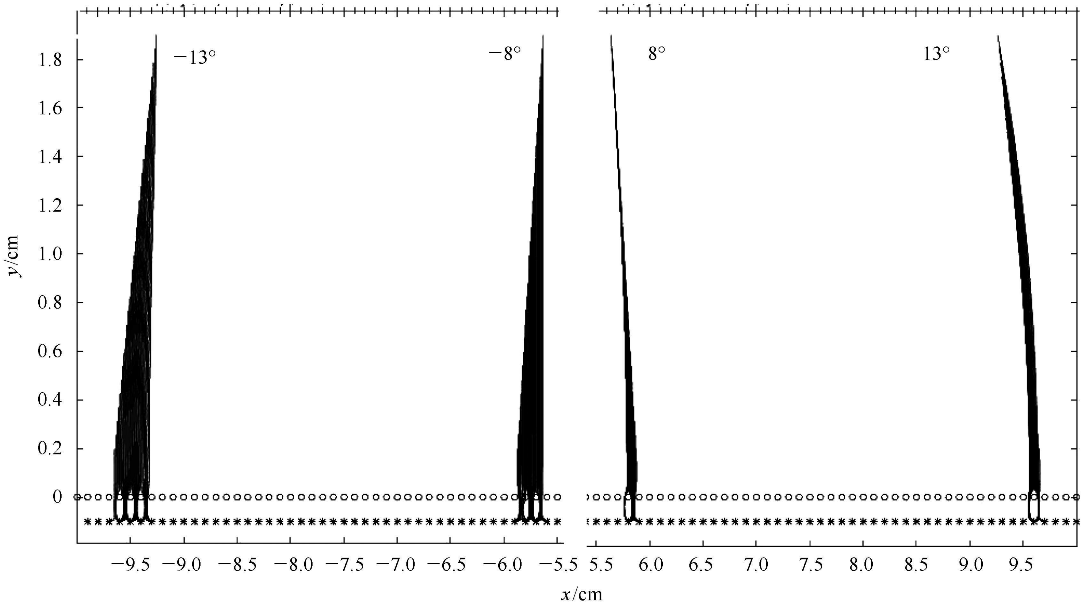

Fig. 4. Electron drift lines from 8° and 13° incident charged tracks. Left: with normal cathode potentials. Right: with non-uniform cathode potentials.

4 Parallax error reduction for micro-pattern detectors

Micro-pattern gas detectors (MSGC, GEM, MicroMegas, etc.) do not use parallel thin wires as the amplification electrodes, so there is no modulation effect like the MWPC. For these detectors, the reduction of parallax broadening after using special cathode potentials can be quantitatively calculated.

4.1 Structures and Garfield modeling

For micro-pattern gas detectors, the drift region is defined as the volume between the cathode and the nearest electrode plane, that is, the microstrip plane (MSGC) or the upper surface of the first GEM film (GEM) or the micro mesh plane (MicroMegas). The electrode plane nearest to the cathode plane can be simply modeled as a flat metal plane. In calculation, a cathode plane made of parallel metal wires and a flat metal plane were used to form the drift region, and the parallax effect was reduced by improving the electric field of the drift region.

Like the simulation for the MWPC, the cathode wires were symmetrically divided into two groups for comparison. One group was normally operated at a same negative high voltage, while the other group applied non-uniform potential according to the distance between the wire and the sample point.

4.2 Simulation results

4.2.1 Electric field and electron drift lines

Equipotential lines similar to Fig.3 can be obtained for the micro-pattern detector. And the characteristics of the electron drift lines are almost the same as those of the MWPC, except for the absence of the anode wire modulation effect.

4.2.2 Position response for different incident angles

The position response of the detector was calculated by recording the positions of the ionized electrons on the anode plane. Obviously, for charged tracks with the same incidence angle, a narrower ionized electron position distribution on the anode plane corresponds to a smaller parallax broadening of the detector.

In the simulation, the position distribution of ionized electrons from charged particle tracks with an incidence angle of ±3°, ±8°, and ±13° was calculated, and the result is shown in Fig. 5. For incidence angles of 3°, 8°, and 13°, the widths (FWHM) of the ionized electron position distributions on the anode

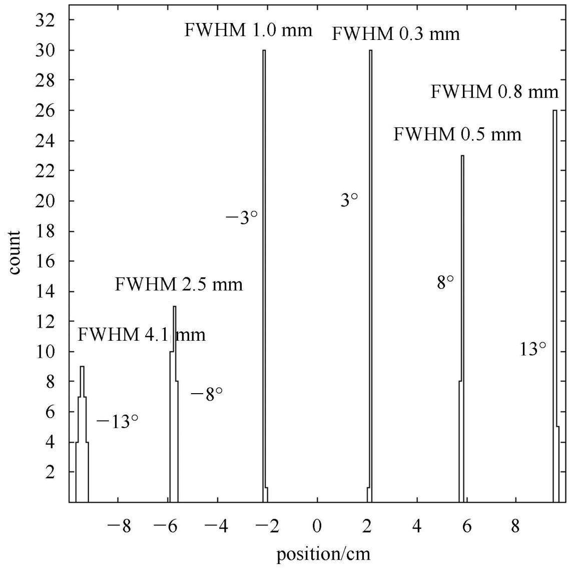

Fig. 5. The electron position distributions on the anode plane, for charged tracks with 3°, 8° and 13° incidence angles. Left: using normal cathode potentials. Right: using non-uniform cathode potentials.

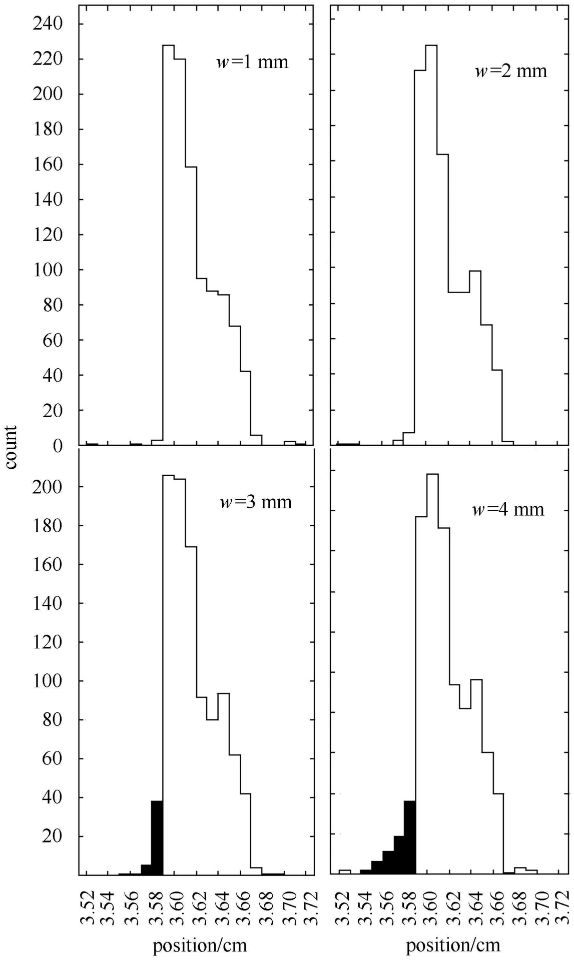

Fig. 6. Position distributions of the ionized electrons from a 5° incidence track, with different cathode wire spacings.

plane were 1.0 mm, 2.5 mm, and 4.1 mm for normal cathode potential region. However, in the special cathode potential region, the widths (FWHM) were reduced to 0.3 mm, 0.5 mm and 0.8 mm respectively. As can be seen, for the maximum incidence angle of 13°, the width (FWHM) of the parallax broadening was reduced to less than 20% of the normal one. So, the use of special cathode potential improves the parallax effect significantly.

4.2.3 Choice of the cathode wire spacing

In the above calculation, the spacings between the cathode wires are 1 mm. Because the potentials of the cathode wires are different from each other, a 1 mm cathode wire spacing means 100 cathode potentials will be needed for a 200 mm×200 mm detector. Though using small cathode wire spacing can obtain a better improvement of the electric field, small cathode wire spacing requires a large number of cathode potentials, and this implies much more complexity in detector manufacture. So, a compromise should be achieved.

Here, the position responses of the detector with cathode wire spacing w of 1 mm, 2 mm, 3 mm and 4 mm are compared. As shown in Fig. 6, for a 5° incidence charged track, the width of the ionized electrons distribution on the anode plane increases if the cathode wire spacing becomes larger than 3 mm. The same phenomena are found for other incidence angles. Therefore, cathode wire spacing of smaller than 3 mm is necessary for the application of this method.

5 Conclusions

The principle of the parallax reduction using non-uniform cathode potentials is introduced. The application of this method on an MWPC and micro-pattern gas detectors, and the impact of the cathode wire spacing are studied. By our calculation, the method significantly reduces the parallax broadening of the planar type gaseous detectors.

In practical application, the parallel wires cathode with non-uniform potential can be used directly in one-dimensional detectors for reduction of the parallax error. For two-dimensional detectors, the parallel wires can be replaced by a series of concentric metal annuli, with each annulus having a potential corresponding to its distance to the sample position.

References

1 Charpak G, Bouclier R, Bressani T et al. Nucl. Instrum. Methods, 1968, **62**: 262

2 Oed A. Nucl. Instrum. Methods A, 1988, **263**: 351

3 Giomataris Y, Rebourgeard Ph, Robert J P et al. Nucl. Instrum. Methods A, 1996, **376**: 29

4 Sauli F. Nucl. Instrum. Methods A, 1997, **368**: 531

5 Aulchenkoa V M, Bukina M A, Drozdetsky A A et al. Nucl. Instrum. Methods A, 2001, **470**: 168

6 Buffeta J C, Clergeaua J F, Cooper R G et al. Nucl. Instrum. Methods A, 2005, **554**: 392

7 Fried J, Harder J A, Mahler G J et al. Nucl. Instrum. Methods A, 2002, **478**: 415

8 Rehak P, Smith G C, Yu B. IEEE Trans. Nucl. Sci. NS, 1997, **44**(3): 651

9 Garfield V R. A Drift-Chamber Simulation Program. Available: http://garfield.web.cern.ch/